Structural Engineering and Mechanics, *Vol. 70, No. 6 (2019) 751-763*
DOI: https://doi.org/10.12989/sem.2019.70.6.751

An efficient and novel strategy for control of cracking, creep and shrinkage effects in steel-concrete composite beams

L. K. Varshney[1a], K. A. Patel[2b], Sandeep Chaudhary[**3] and A. K. Nagpal[1c]

[1]*Department of Civil Engineering, Indian Institute of Technology Delhi, New Delhi 110016, India*
[2]*Department of Civil Engineering, Institute of Infrastructure, Technology, Research And Management (IITRAM), Ahmedabad 380026, India*
[3]*Discipline of Civil Engineering, Indian Institute of Technology Indore, Simrol, Indore 453552, India*

(Received July 23, 2018, Revised March 16, 2019, Accepted March 19, 2019)

Abstract. Steel-concrete composition is widely used in the construction due to efficient utilization of materials. The service load behavior of composite structures is significantly affected by cracking, creep and shrinkage effects in concrete. In order to control these effects in concrete slab, an efficient and novel strategy has been proposed by use of fiber reinforced concrete near interior supports of a continuous beam. Numerical study is carried out for the control of cracking, creep and shrinkage effects in composite beams subjected to service load. A five span continuous composite beam has been analyzed for different lengths of fiber reinforced concrete near the interior supports. For this purpose, the hybrid analytical-numerical procedure, developed by the authors, for service load analysis of composite structures has been further improved and generalized to make it applicable for composite beams having spans with different material properties along the length. It is shown that by providing fiber reinforced concrete even in small length near the supports; there can be a significant reduction in cracking as well as in deflections. It is also observed that the benefits achieved by providing fiber reinforced concrete over entire span are not significantly more as compared to the use of fiber reinforced concrete in certain length of beam near the interior supports in continuous composite beams.

Keywords: composite beam; cracking; creep; fiber reinforced concrete; shrinkage

1. Introduction

In recent years, steel-concrete composition (Fig. 1) has attained lot of significance owing to its mutual functional advantages, economy as well as rapid construction ability. The steel and concrete are effectively utilised to carry the tensile and compressive stresses respectively in composite beams. This results in higher flexural rigidity and lesser bending stresses and deflections. On contradictory, the cracking and time-effects in concrete slab may reduce the rigidity and hence increase the deflection (Wang *et al.* 2011, Mohammadhassani *et al.* 2013a, b).

Since the concrete is not much capable to resist the tensile stresses, it may crack at the time of first (instantaneous) loading at the hogging moment regions (Ramnavas *et al.* 2017). In addition to the first cracking, the time-effects (creep and shrinkage) in concrete under sustained load, play a considerable role owing to their progressive effects on the cracking though out the life of the structures. These effects lead to change in the distribution of stresses as well as enhancement of deflections (Pendharkar *et al.* 2010, 2011). Therefore, development of various strategies to minimize the effects of cracking, creep and shrinkage is desirable in order to enhance the serviceability and durability performance of the structures.

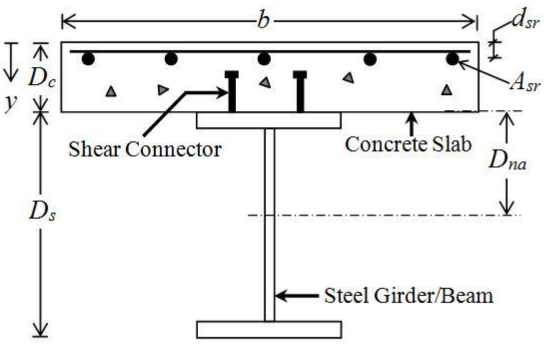

Fig. 1 A typical composite cross-section

Utilization of steel fibers in concrete can be a strategy for controlling cracking in concrete slab of composite structures. Application of steel fiber reinforced concrete (FRC) in the zone near the interior supports of a continuous beam (where cracking occurs due to the hogging moment), crack opening and its propagation can be significantly controlled because of its excellent resistance capacity against cracking and its propagation. The resistance capability of steel FRC is achieved by the holding ability of fibres in concrete matrix.

*Corresponding author, Ph.D.
E-mail: schaudhary@iiti.ac.in
[a] Ph. D.
E-mail: lalitamu@yahoo.co.in
[b] Ph. D.
E-mail: iitd.kashyap@gmail.com
[c] Ph. D.
E-mail: aknagpal@civil.iitd.ac.in

http://www.techno-press.com/journals/sem&subpage=7
ISSN: 1225-4568 (Print), 1598-6217 (Online)

Extensive literature (Swamy and Stavrides 1979, Chern and Young 1989, 1990, Grzybowski and Shah 1989, 1990, Sargaphuti *et al.* 1993, Zollo 1997, Nataraja *et al.* 1999, Olesen 2001, Zhang 2003, Haddad and Smadi 2004, Kwon and Shah 2008, Wang and Dai 2013, Johnston 2014, Zhao *et al.* 2015, Tang 2017) is available on the influence of inclusion of steel fibers in concrete on various properties. Swamy and Stavrides (1979) have studied the effect of fiber reinforcement on concrete cracking and restrained shrinkage. They observed that the drying shrinkage can be reduced by up to twenty percent through the application of fibers in concrete. They further concluded that the fibers contained specimens can resist the shrinkage-induced stresses even after eight to twelve months. Chern and Young (1989) studied the effect of steel fiber on the compressive strength, elastic modulus, creep and shrinkage. The important conclusions were (i) concrete having higher fiber content gives higher compressive strength and elastic modulus in later age (more than 4 days); (ii) the reduction in creep- and shrinkage-induced stresses are more for higher fiber content; and (iii) inclusion of steel fibers leads to reduce in deformations at later age. Again, Chern and Young (1990) studied the factors influencing drying shrinkage of SFRC. The test results indicated that the optimum volume content of fibers to reduce shrinkage of concrete is less than 2%.

Grzybowski and Shah (1989) proposed an analytical model which enables progressive cracking development considering many of the key parameters in fiber reinforced concrete (FRC) subjected to restrained shrinkage. Zhang (2003) studied the effect of fibers on creep in FRC based composites by developing an analytical model. The studies reveal that the creep-induced strain in the concrete with FRP is greatly dependent on moduli of elasticity of fiber and its geometric properties. Kwon and Shah (2008) have carried out studies for prediction of initiation of time of cracking and crack width subjected to time of concrete with and without fibers. FRC may thus be used as an appropriate material for controlling crack, creep and shrinkage effects in concrete slab of composite beams.

Some studies are available in literature for the short-term (instantaneous) and long-term behaviour of SFRC structural elements. Tan *et al.* (1994) performed the experiments for studying the short-term and long-term deflections of SFRC beams. An analytical method based on effective moment of inertia approach has been further proposed for the prediction of both the instantaneous and long-term deflections. Later, Tan *et al.* (1995) studied the cracking characteristics of SFRC beams under first and long duration loadings. An analytical method has been proposed for the estimation of maximum crack width under instantaneous loading. Furthermore, a semi-empirical expression for the long-term crack widths prediction under sustained loads is also proposed. The results showed that the utilisation of steel fibers considerably reduced the maximum crack widths in beams made from steel FRC. Under ten years sustained loading period, Saha and Tan (2005) have concluded that the use of 2% steel fiber content concrete leads to reduction in maximum crack width and long-term deflections of 58% and 34%, respectively. Sryh (2017) has studied the long-term flexural performance of cracked reinforced concrete beams incorporating steel fibers and recycled aggregate. The studies reported that the degradation in properties owing to use of recycled aggregates can be balanced by utilisation of fibers in concrete.

On the other hand, very limited studies are available for crack control in composite structures incorporating time dependent (creep and shrinkage) effects. Kwak and Seo (2002) presented a study on control of shrinkage induced cracking at the intermediate supports of continuous bridges made from pre-cast pre-stressed concrete girders. They recommended providing a bearing at one end of the intermediate span in order to minimize the effects of transverse cracking at hogging moment regions. Ryu *et al.* (2005) focused on identification of factors which controls the cracking at interior supports of a continuous composite girder having prefabricated concrete slabs. They concluded that the transverse reinforcement arrangement is the most influencing factor to the crack spacing. Further, Ryu *et al.* (2007) have conducted the full scale experiments in order to control the cracks of a two span continuous bridge. Provision of loop jointed prefabricated slabs was found to reduce the width of crack arising due to hogging moment.

Chaudhary *et al.* (2009) and Varshney *et al.* (2013) have carried out numerical studies for controlling the creep and shrinkage effects in composite structures having pre-cast concrete slab. They provided a strategy, of simply delaying the time of mobilization of composite action between the slab and the steel section, for drastic reduction in moments and deflections. Lin *et al.* (2014) have experimentally proven that the inclusion of steel fibers is beneficial for controlling the crack spacing and width and thus enhancing the mechanical performance of composite of beams. Through extensive experiments, Gholamhoseini *et al.* (2016) concluded that the application of steel FRC leads to control the cracking, creep and shrinkage-induced strains and improvement of strength and serviceability performance of two span continuous composite slabs. Hamoda *et al.* (2017) have conducted the experiments and observed that the provision of ultra-high performance FRC closure strip at the interior support of two span high performance FRC continuous beams gives better cracking control.

From the above detailed literature review, it can be seen that no comprehensive numerical studies are available for the FRC effects in controlling cracking in concrete slab of composite beams and hence improved performance of steel-concrete composite beams considering creep and shrinkage in concrete. Further, a systematic study is required for the influence of different lengths (along the span) of FRP near the interior supports of service load behaviour of composite beams.

Herein, an efficient and novel strategy has been proposed by use of FRC near the interior supports of continuous steel-concrete composite beams. Numerical study is carried out for the control of cracking, creep and shrinkage effects in composite beams subjected to service load. A five span continuous composite beam has been analyzed for different lengths of FRC near the interior

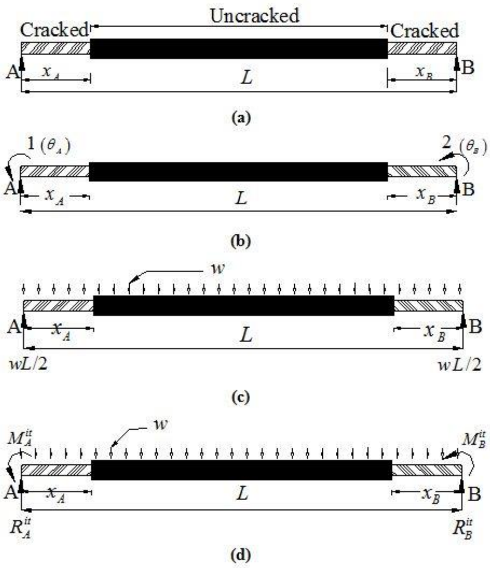

Fig. 2 Cracked span length beam element having (a) cracked and uncracked zones, (b) degrees of freedom at the ends, (c) their releases and (d) applied uniformly distributed load and forces at the ends (Chaudhary *et al.* 2007)

supports. For this purpose, the hybrid analytical-numerical procedure (Chaudhary *et al.* 2007) for service load analysis of composite structures has been further improved and generalized to make it applicable for composite beams having span of different material properties. The results for the composite beams containing steel FRC applied in different lengths in the hogging moment regions are also compared with those for conventional concrete (no steel fibers content). The effects owing to inclusion of steel FRC on crack lengths, bending moments and deflections are studied.

2. Hybrid analytical-numerical procedure

A hybrid analytical-numerical procedure (Chaudhary *et al.* 2007) has been developed by authors for studying the time-dependent behavior of composite beams subjected to service load. The procedure incorporates the effects caused from cracking, creep and shrinkage in concrete slab. As stated earlier, the procedure is quite computationally efficient as no discretisation is required along the length and across the cross-section. In order to keep the procedure analytical at the element level, a cracked span length beam is idealized. The span length beam element is bifurcated into two cracked zones at the ends and an uncracked zone in the middle of the span as shown in Fig. 2 to incorporating cracking. Herein, the element considers the effect of cracking only due to moment and neglects its effect due to shear and torsion.

Assuming closely spaced shear connectors, slip between the steel girder and concrete slab has been ignored. When the working stress of the concrete slab at top fibre exceeds the tensile strength of the concrete, f_t, the entire concrete cross-section is assumed to be cracked.

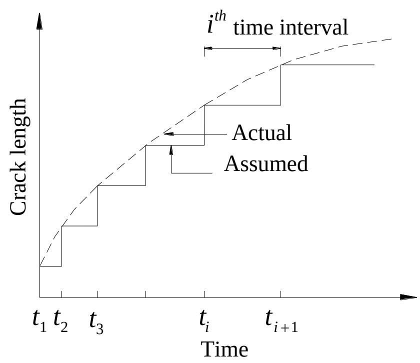

Fig. 3 Cracked length updating for progressive cracking (Chaudhary *et al.* 2007)

In the range of serviceability, the concrete is assumed to behave as linear-elastic material in compression as well as in tension prior to cracking. In order to predict the performance accurately, the effect of tension stiffening is considered for the cracked zone. For this purpose, the cracked zone is divided into two states, cracked and uncracked. Only the sections of steel girder and embedded reinforcement of concrete slab are considered for the cracked state.

The contributions of the cracked and uncracked states are denoted by interpolation coefficients, ζ and $\eta\ (=1-\xi)$ respectively. Eurocode 2 (1992) suggests the expression for the evaluation of the interpolation coefficient as $\xi = 1-\kappa\left(f_t/\sigma_{un}\right)^2$ where, κ is the reduction factor which relates tension stiffening effect with time and σ_{un} is the tensile stress at the top fiber.

Steel is considered as linear-elastic material for both tension and compression assuming the stresses under the service load to be below yielding stress.

The procedure carries the analysis in two phases. In the first (instantaneous) phase, an iterative process is used. In the second (time-dependent) phase, the time is divided into a number of small increments in order to consider the progressive cracking.

In the second phase, the crack length is assumed to be constant within the increment as shown in Fig. 3. To incorporate the creep and shrinkage effects, the age-adjusted effective modulus method (AEMM), developed by Bazant (1972), is utilised in the procedure.

In order to minimise the computational efforts, the closed form expressions for flexibility matrix coefficients (w.r.t. releases 1 and 2) of the beam element (Fig. 2) are given as (Chaudhary *et al.* 2007)

$$f_{11} = \frac{1}{3L^2}\begin{bmatrix} S_{un}^{x}\left(\eta_A L^3 - \xi_B x_B{}^3 + \xi_A y_A{}^3\right) \\ +S_{cr}^{x}\left(\xi_A L^3 + \xi_B x_B{}^3 - \xi_A y_A{}^3\right) \end{bmatrix} \tag{1}$$

$$f_{12} = f_{21} = \frac{1}{6L^2}\begin{bmatrix} \xi_A x_A{}^2\left(2x_A - 3L\right) \\ +\xi_B x_B{}^2\left(2x_B - 3L\right) \end{bmatrix}\left(S_{cr}^{x} - S_{un}^{x}\right) - \frac{S_{un}^{x} L}{6} \tag{2}$$

$$f_{22} = \frac{1}{3L^2}\begin{bmatrix} S_{un}^{x}\left(\eta_B L^3 - \xi_A {x_A}^3 + \xi_B {y_B}^3\right) \\ +S_{cr}^{x}\left(\xi_B L^3 + \xi_A {x_A}^3 - \xi_B {y_B}^3\right)\end{bmatrix} \tag{3}$$

where, ξ_A and η_A are the interpolation coefficients for the cracked zone at the end A; ξ_B and η_B are the interpolation coefficients for the cracked zone at the end B; x_A , x_B are the crack lengths at ends A and B respectively; $y_A = L - x_A$; $y_B = 1 - x_B$; and the quantities S_{un}^{x} and S_{cr}^{x} are calculated using the uncracked and cracked states properties (Chaudhary *et al.* 2007). The coefficients of stiffness matrix, $[k]$ corresponding to degrees of freedom 1, 2, 3 and 4 are obtained as (Patel *et al.* 2016)

$$[k]=\begin{array}{cc} & \begin{array}{cccc} \quad 1 \quad & \quad 2 \quad & \quad 3 \quad & \quad 4 \quad \end{array} \\ \begin{array}{c} 1 \\[4ex] 2 \\[4ex] 3 \\[5ex] 4 \end{array} & \begin{bmatrix} k_{11} & k_{12} & \dfrac{(k_{11}+k_{12})}{L} & \dfrac{-(k_{11}+k_{12})}{L} \\ k_{21} & k_{22} & \dfrac{(k_{21}+k_{22})}{L} & \dfrac{-(k_{21}+k_{22})}{L} \\ \dfrac{(k_{11}+k_{12})}{L} & \dfrac{(k_{21}+k_{22})}{L} & \dfrac{\begin{pmatrix} k_{11}+k_{12} \\ +k_{21}+k_{22}\end{pmatrix}}{L} & -\dfrac{\begin{pmatrix} k_{11}+k_{12} \\ +k_{21}+k_{22}\end{pmatrix}}{L} \\ \dfrac{-(k_{11}+k_{12})}{L} & \dfrac{-(k_{21}+k_{22})}{L} & -\dfrac{\begin{pmatrix} k_{11}+k_{12} \\ +k_{21}+k_{22}\end{pmatrix}}{L} & \dfrac{\begin{pmatrix} k_{11}+k_{12} \\ +k_{21}+k_{22}\end{pmatrix}}{L^2} \end{bmatrix} \end{array} \tag{4}$$

where,

$$k_{11} = f_{22} / \left(f_{11} f_{22} - f_{12} f_{21} \right);$$
$$k_{12} = k_{21} = - f_{12} / \left(f_{11} f_{22} - f_{12} f_{21} \right);$$
$$k_{22} = f_{11} / \left(f_{11} f_{22} - f_{12} f_{21} \right).$$

Similarly, the closed form expressions for end displacements, crack lengths and mid-span deflection may be obtained from the Chaudhary *et al.* (2007).

The results from the hybrid procedure have been verified by comparison with those from the experimental results available in literature (Chaudhary *et al.* 2007).

3. Improvement of hybrid procedure for continuous composite beams having fiber reinforced concrete at near interior supports

A typical five span continuous composite beam and its bending moment diagram subjected to a service load are shown in Fig. 4a, b. There would be hogging moments at the interior supports of the continuous beam. Due to this hogging moment at interior supports, cracks may develop in the concrete slab of the composite beam on both sides of the interior supports (Fig. 4(c)) as concrete has very less tensile strength.

To control this cracking in the zone near each interior support of the continuous composite beam, it is proposed to use the Fiber Reinforced Concrete (FRC) instead of Conventional Concrete (CC) in partial beam length on both side of interior supports of the beam (Fig. 4(d)) as inclusion of fibers in concrete increases the tensile as well as compressive strength and also reduces creep and shrinkage effects (Malmberg 1978, Ashour *et al.* 2000).

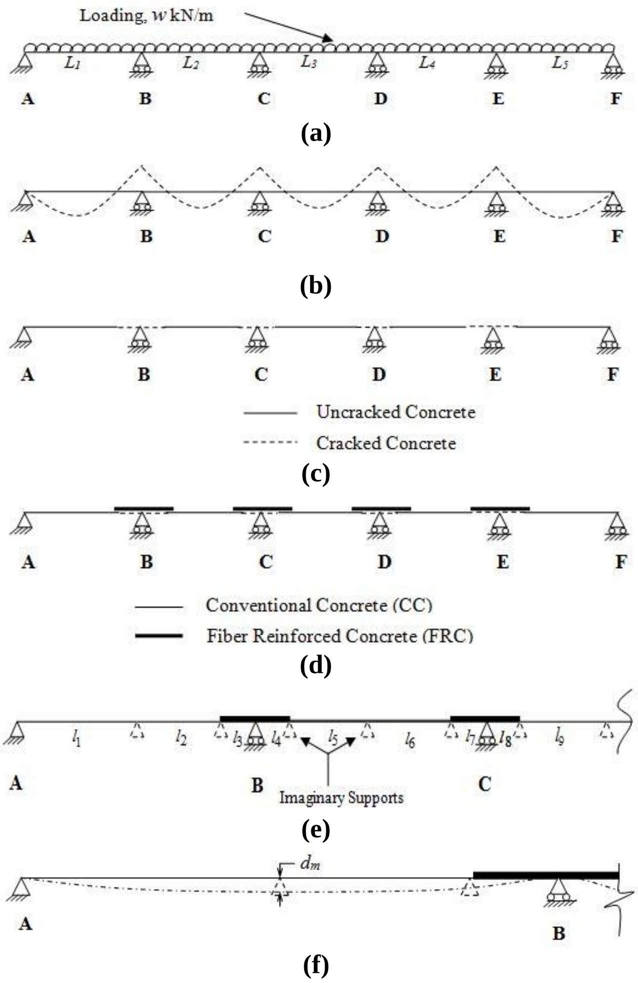

Fig. 4 (a) A typical five span continuous composite beam, (b) typical bending moment, (c) concrete cracking near interior supports due to hogging moment, (d) use of FRC on both sides of interior supports, (e) details of five span composite beam divided in eighteen spans and (f) enlarged span AB for calculating mid-span deflection

When the FRC is provided in partial length of the spans, there would be difference in properties of the material in the same span of composite beam as the properties of FRC and CC are different from each other. It may be noted the, the hybrid procedure is applicable for spans having same material throughout the span; therefore, the spans having partial length of FRC are to be divided into spans having same properties for analysis by the hybrid procedure. For this, the imaginary supports have been provided where ever there is change in properties (Fig. 4(e)) or where ever the deflections are required to be obtained in the continuous composite beam (for e.g. at the mid-span length of the beam so that the mid-span deflection can be easily obtained by just obtaining the settlement of imaginary supports in case of continuous composite beam).

Each exterior span is supported by the exterior and penultimate supports. There is no moment occurrence at the exterior support hence no cracking develop at the support as shown in Figs. 4(a)-(b). At the penultimate support, the cracking may occur due to hogging moment (Figs. 4(a)-(b)). Therefore, each exterior span is divided into three spans through two imaginary supports (i) at mid-span for deflection calculation and (ii) at the junction of FRC and CC as different material properties (Fig. 4(e)). Similarly, each interior span is supported by two interior supports and hogging moments and cracking may occur at both the supports as shown in Figs. 4(a)-(b). Therefore, each interior span is divided into four spans through three imaginary supports (i) at mid-span for deflection calculation; (ii) at both the junctions of FRC and CC as different material properties (Fig. 4(e)).

Consider a five span continuous composite beam. The FRC has been provided near interior supports as interior supports are highly prone to cracking due to hogging moments. The five spans of continuous composite beam may be divided into eighteen spans (exterior spans are divided into three spans and interior spans are divided into four spans). Thus, five span continuous composite beams with FRC near interior supports can be modeled as a limiting case of single storey eighteen bay frame having one hinge support and eighteen roller supports (out of which six supports are actual and thirteen supports are imaginary as shown in Fig. 4(e)). The actual supports of the beam are assumed to have a large area, negligible moment of inertia and negligible length, whereas, the imaginary supports of the beam are assumed to have a negligible area, negligible first moment of area, negligible second moment of area and negligible length.

4. Numerical study

As stated in the introduction, no studies are available for the FRC effects in controlling cracking in concrete slab of steel-concrete composite beams considering creep and shrinkage in concrete. Herein, a numerical study has been carried out for the continuous composite beam.

As stated earlier, due to the hogging moment (higher the cracking moment) near the interior supports, cracking of the concrete slab may take place. To control this cracking in concrete slab of composite beam, an efficient and novel strategy is proposed hereby by providing the steel FRC in the hogging moment regions only which are the potential zone for cracking i.e. near all the interior supports in case of continuous composite beam instead of providing the FRC in the complete beam length.

Herein, numerical studies are presented for a five span continuous composite beam. Studies are carried out for different cases of decks i.e. (i) CC slabs over entire spans (Fig. 5(a)), (ii) FRC slabs over entire spans (Fig. 5(b)), (iii) FRC in 15% of the span lengths instead of CC on both side of each interior support, F15 (Fig. 5(c)), and (iv) FRC in 25% of the span lengths instead of CC on both side of each interior support, F25 (Fig. 5(d)). For each case, four different magnitudes of load are considered i.e. (i) $w=w_{cr}$, (ii) $w=1.25w_{cr}$, (iii) $w=1.50w_{cr}$, and (iv) $w=2.0w_{cr}$, where w_{cr} is the cracking load at which the first crack occurs in continuous composite beam. In case of FRC, the amount of fiber is assumed to be 2%. It is well established

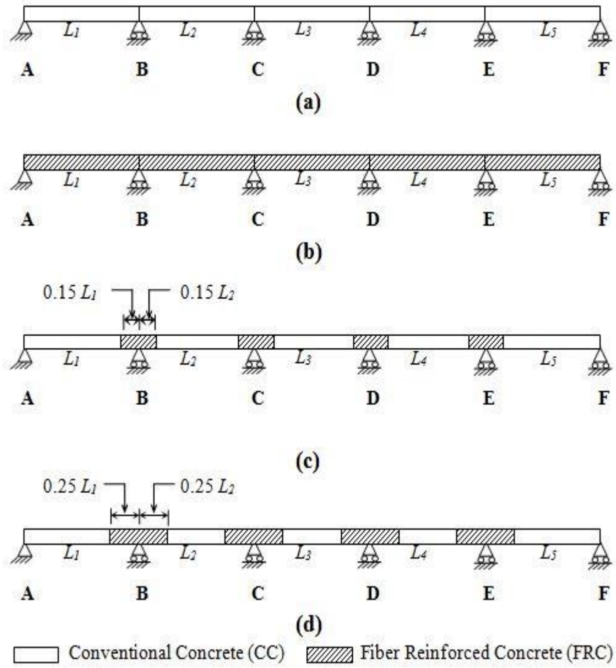

Fig. 5 Different cases of a five span continuous composite beam for numerical study

from the literature that the addition of steel fibers in concrete increases the compressive strength, modulus of rupture and reduces creep and shrinkage in concrete. For concrete containing 2% of fiber volume, the compressive strength and modulus of rupture of concrete may be assumed to increase by 40% and 50% respectively (Ashour *et al.* 2000) and the creep and shrinkage coefficient may be assumed to decrease by 17.88% (Zhang 2003) and 17.77% (Malmberg 1978) respectively.

A continuous composite beam of five spans, EB1 (Fig. 4(a), $L_1 = L_2 = L_3 = L_4 = L_5 = 7.0$ mm) is considered. Similar composite cross-section for all the spans (AB, BC, CD, DE and EF) is taken. For steel girder, the rolled section of 356×171 UB 67 having total depth, D_s = 364 mm is considered. The area, A_s and second moment of area about its neutral axis, I_s of steel girder are calculated as 8530 mm^2 and 1.9483×10^8 mm^4 respectively. The dimensions and reinforcement details of the concrete slab are: depth, D_c = 125 mm; width, b = 1100 mm; area of reinforcement, A_{sr} = 508 mm^2; and cover for top fiber, d_{sr} = 15 mm. The material properties are: cubic compressive strength of concrete at 28 days, f_{ck} = 30 N/mm^2; modulus of elasticity of steel, E_s = 2.05×10^5 N/mm^2; and time of mobilization of composite action between concrete panel and steel section, t_1 = 7 days. The instantaneous and time-dependent properties of the concrete are evaluated in accordance with CEB-FIP (1990) and its update (FIB 1999). Considering material and cross-sectional properties, the load, w_{cr} at which cracking first occurs at penultimate support B of the continuous composite beam is calculated as 16 kN/m. The relative humidity and mean temperature are taken as 50% and 20 ºC respectively. A total time-

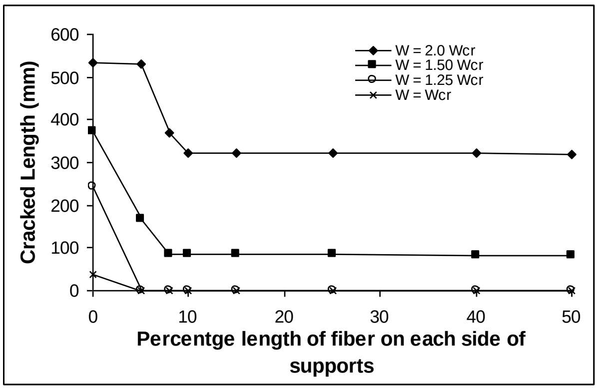

Fig. 6 Variations of crack length in span AB

duration of 20,000 days is assumed and it is divided into 20 time intervals.

For studies of the continuous composite beam having FRC in 15% and 25% of the span length instead of CC on both side of each interior supports, as discussed earlier, five spans have been divided into eighteen spans (i.e. exterior spans into three spans and interior spans into four spans as shown in Fig. 4(e)) by providing imaginary supports just below the point of junction of FRC with CC and also at the point where deflection is to be determined i.e. at the mid-span length. The use of FRC is in partial length of the beam near the interior supports therefore the properties of FRC and CC need to be assigned separately in required portion of beam. For this purpose, the continuous beam has been divided into a number of spans as surlier stated pattern. The mid-span deflection for a span of the beam is obtained by settlement of the imaginary support provided at that point (Fig. 4(f)).

Variations of crack length for different percentage of FRC in the span length instead of CC on both sides of each joint are shown in Fig. 6 for four loading cases stated above. For the loading cases, $w = w_{er}$ and $w = 1.25w_{cr}$, cracking of beam is prevented completely by using a very less percentage, say 5% FRC instead of CC in span length on both sides of interior supports. While for the loading cases, $w = 1.50w_{cr}$ and $w = 2.0w_{cr}$, cracking of beam is controlled upto a certain extent only even by using FRC instead of CC concrete in complete span length. This shows that it would not be much beneficial to use the FRC instead of CC in complete span length of the continuous composite beam to control the crack length as crack lengths are same for FRC in complete span length and FRC in 10% span length on each side of the interior supports for each considered loading cases as stated above.

However, on application of very less FRC, say 5% on each side of the interior supports, cracks may develop in the CC slab portion (as shown in Fig. 7) adjacent to the FRC slab portion thus defeating the purpose of providing FRC. This is due to the fact that FRC has sufficient strength against crack propagation but CC has very less strength against crack propagation, so when higher loads are applied then some CC portion (beyond the FRC portion) comes under high hogging moment and cracks may develop in the CC portion, although away from interior supports as shown in Fig. 7.

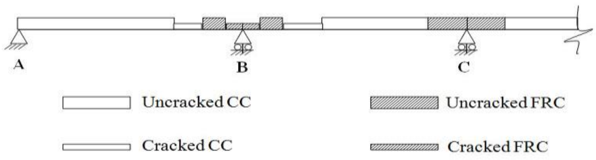

Fig. 7 Cracking pattern for small length (i.e. 0.05L) of FRC in span length

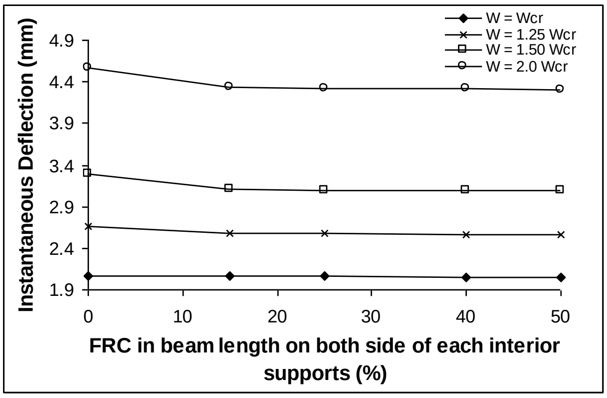

Fig. 8 Variation of instantaneous mid-span deflection of span AB

Hence, it would be beneficial to put some minimum percentage of FRC in span length instead of CC on both sides of the interior supports to control the cracking of slab upto maximum extent. Therefore, studies are carried out here for FRC in 15% and 25% of the span lengths instead of CC on both side of each interior support and results are compared with the CC slabs over entire span and FRC slabs over entire span.

Variations of instantaneous mid-span deflection of span AB with FRC on both sides of interior supports in continuous composite beam for different loading cases are shown in Fig. 8. It is noted that for smaller length of FRC (from 0 to 15%), there is more variation in instantaneous deflection for higher loading case (i.e. $w=1.50w_{cr}$ and $w=2.0w_{cr}$) because of the effects of cracking control as well as the increased stiffness in case of FRC. However, there is a slight change in instantaneous deflection for smaller loading case (i.e. $w=w_{cr}$ and $w=1.25w_{cr}$) as there is very small cracking, which can be controlled by using very low FRC and there is effect of only increased stiffness in case of FRC. It is further reported that there is a slight variation in instantaneous mid-span deflection on using FRC higher than 15% as cracking is constant (Fig. 6) and there is effect of only increased stiffness of FRC.

Variations of change in mid-span deflection $d_m^t - d_m^{it}$ of span AB with FRC in beam length on both sides of interior supports for different loading cases are shown in Fig. 9. It is observed that for low use of FRC (from 0 to 15%), there is more variation in change in mid-span deflection $d_m^t - d_m^{it}$ for higher loads (i.e. $w=1.50w_{cr}$ and $w=2.0w_{cr}$). Then, further there is a slight variation in change in mid span deflection on using FRC in more than 15% beam length.

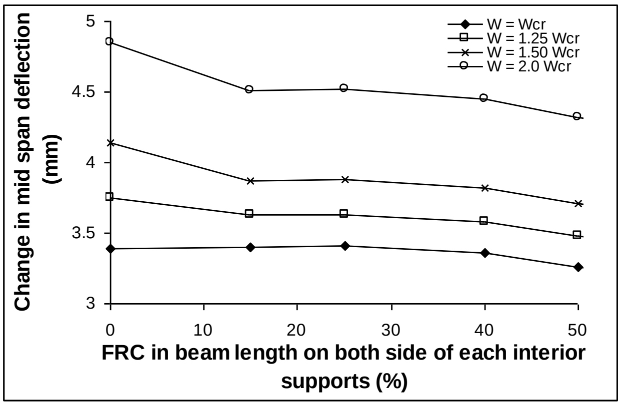

Fig. 9 Variation of change in mid-span deflection ($d_m^t - d_m^{it}$) of span AB

Time-dependent variations of mid-span deflection for span AB are shown in Fig. 10 for all the loading cases. The values are also given in the Table A1 of Appendix A for greater clarity. It is observed that total deflection is less for beam having complete FRC in comparison for beam having complete CC as expected. Further, it is noted that as the loading is increased from $w = w_{cr}$ to $w = 2.0w_{cr}$, the effect of using FRC, instead of CC in partial beam length on both side of interior supports, is more. This is due to the fact that in case of smaller loading (i.e. $w = w_{cr}$, $w = 1.25w_{cr}$), crack length is controlled completely by just using a very less FRC portion in beam length (Fig. 6), while at increased load magnitudes, there is more cracking and therefore, there is more effect of using FRC portions in controlling the cracking.

Variations of instantaneous bending moment at right end of span AB with FRC on both sides of interior supports in continuous composite beam for different loading cases are shown in Fig. 11. It is noted that for smaller lengths of FRC (from 0 to 15%), there is more variation in instantaneous bending moment for higher loading case (i.e. $w = 1.50w_{cr}$ and $w = 2.0w_{cr}$) because the amount of cracking controlled is large. Whereas, there is a small change in instantaneous bending moment for smaller loading case (i.e. $w = w_{cr}$ and $w = 1.25w_{cr}$) owing to less cracking even when there is no FRC. It is further reported that there is no longer change in instantaneous bending moment on use of FRC in more than 15% of span length as no change in cracked lengths is observed (Fig. 6) for both smaller and higher loading cases.

Variations of change in bending moment ($M^t - M^{it}$) at right end of span AB with FRC on both sides of interior supports in continuous composite beam for different loading cases are shown in Fig. 12. It is reported that the change in hogging moment initially increases for change in length of FRC portion from 0 to 15% and then decreases for higher lengths of FRC portion, though the change is still higher than complete CC portion. There are two factors influencing the change in bending moment. First, owing to greater uncracked length, the portion causing creep and shrinkage increases, thereby increasing the time-dependent change in bending moment. Second, the creep and

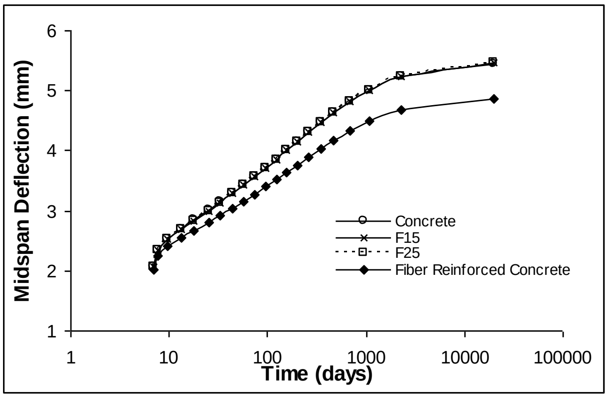

(a)

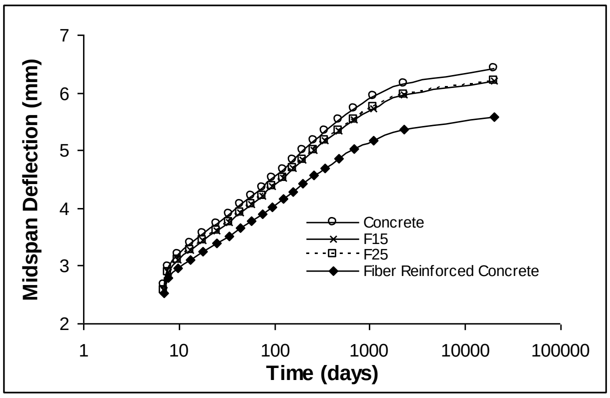

(b)

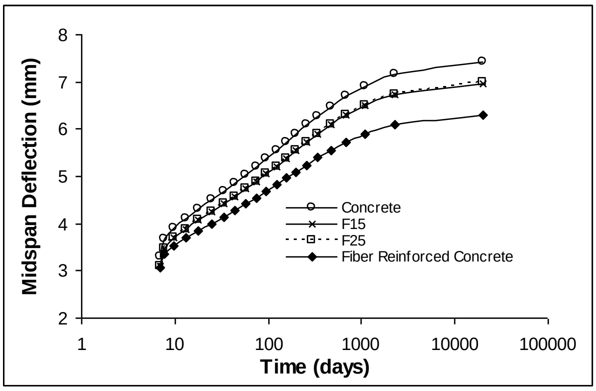

(c)

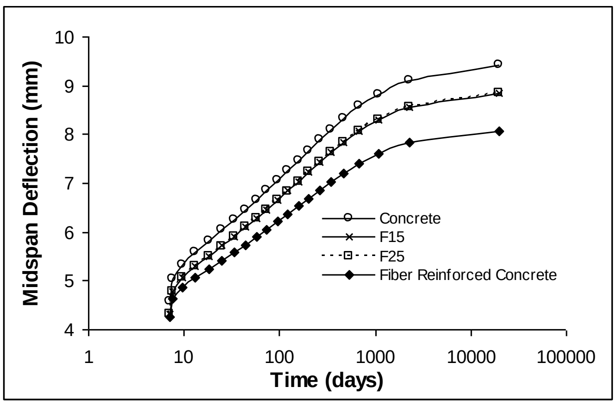

(d)

Fig. 10 Time-dependent variation of mid-span deflection for span AB: (a) $w = w_{er}$, (b) $w = 1.25w_{cr}$, (c) $w = 1.50w_{cr}$ and (d) $w = 2.0w_{cr}$

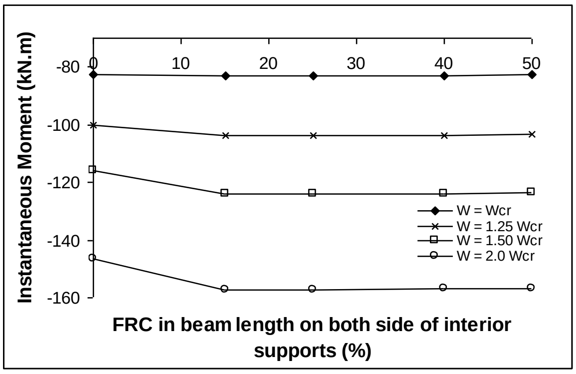

Fig. 11 Variation of instantaneous bending moment at right end of span AB

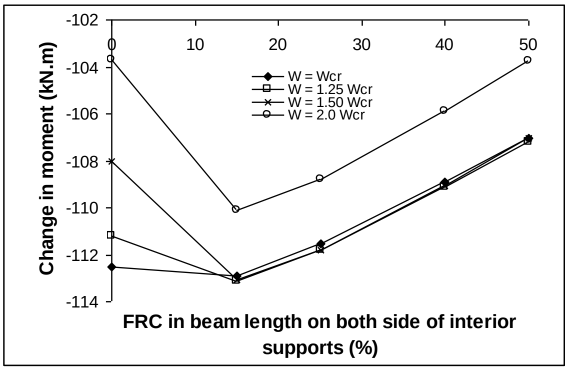

Fig. 12 Variation of change in bending moment ($M^t - M^{it}$) at right end of span AB

shrinkage is reduced in the FRC as compared to CC, thereby decreasing the time-dependent change in bending moment. For, smaller length of FRC, the first factor is predominant whereas for its greater length, the second factor becomes predominant.

Time-dependent variations of bending moment at right end of span AB (at support B) are shown in Fig. 13 for all the loading cases. The values are also given in the Table A2 of Appendix A for greater clarity. It is observed that in case of smaller loads (i.e. $w = w_{er}$, $w = 1.25w_{cr}$), the beam having complete CC has higher long term bending moments at support B as compared to beam having complete FRC. The opposite happens in case of higher loads (i.e. $w = 1.50w_{cr}$, $w = 2.0w_{cr}$). The instantaneous bending moment of beam having complete CC is smaller than that for complete FRC at higher loads owing to moment redistribution. This leads to smaller total bending moment even though the time-dependent change is higher. Whereas, in case of smaller loads, the redistribution of instantaneous bending moment does not take place or it is very small. On contradictory, the beam with complete CC have lower long term bending moments at mid of span AB as compared to beam having complete FRC can be expected for both the loading cases, smaller loads (i.e. $w = w_{er}$, $w = 1.25w_{cr}$), and higher loads (i.e. $w = 1.50w_{cr}$, $w = 2.0w_{cr}$).

Time-dependent variations of bending moment at right end of span CD (at support D) are shown in Fig. 14 for all the loading cases. The values are also given in the Table A3 of Appendix A for greater clarity. It is observed that the beams with CC over entire span length have higher long term bending moment at support D as compared to beam having complete FRC. This is due to greater creep and shrinkage in CC than in FRC. As expected, contradictory variation in long term bending moment can be seen at mid of span CD or both the loading cases.

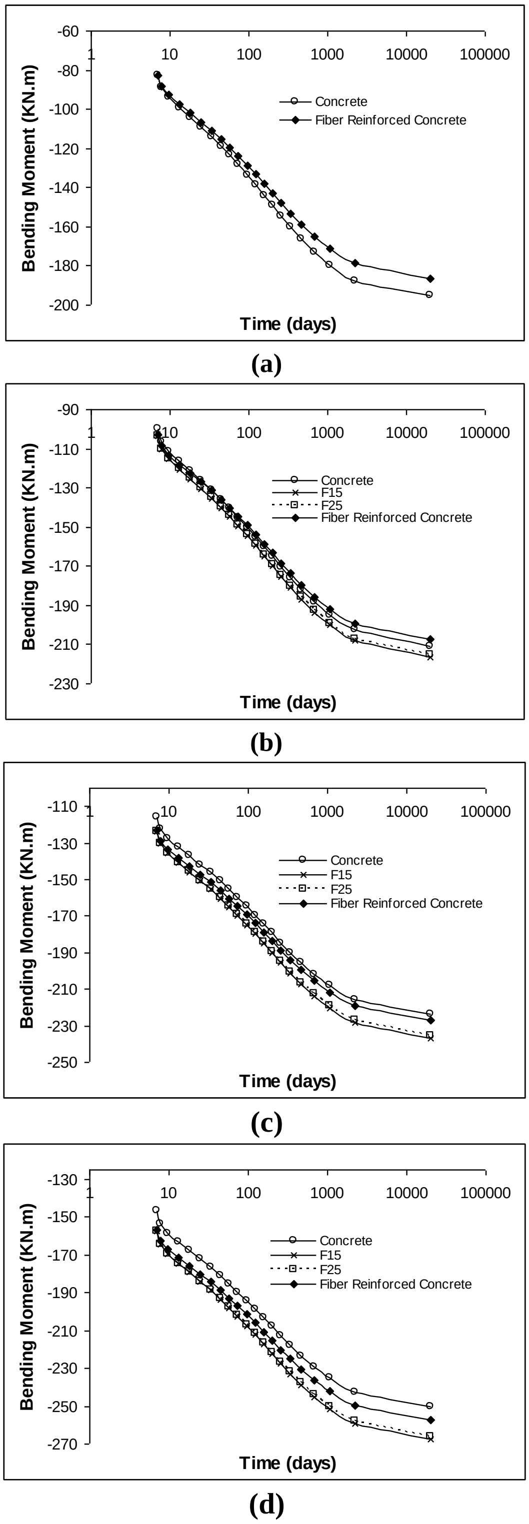

Fig. 13 Time-dependent variation of bending moment at right end of span AB: (a) $w = w_{er}$, (b) $w = 1.25w_{cr}$, (c) $w = 1.50w_{cr}$ and (d) $w = 2.0w_{cr}$

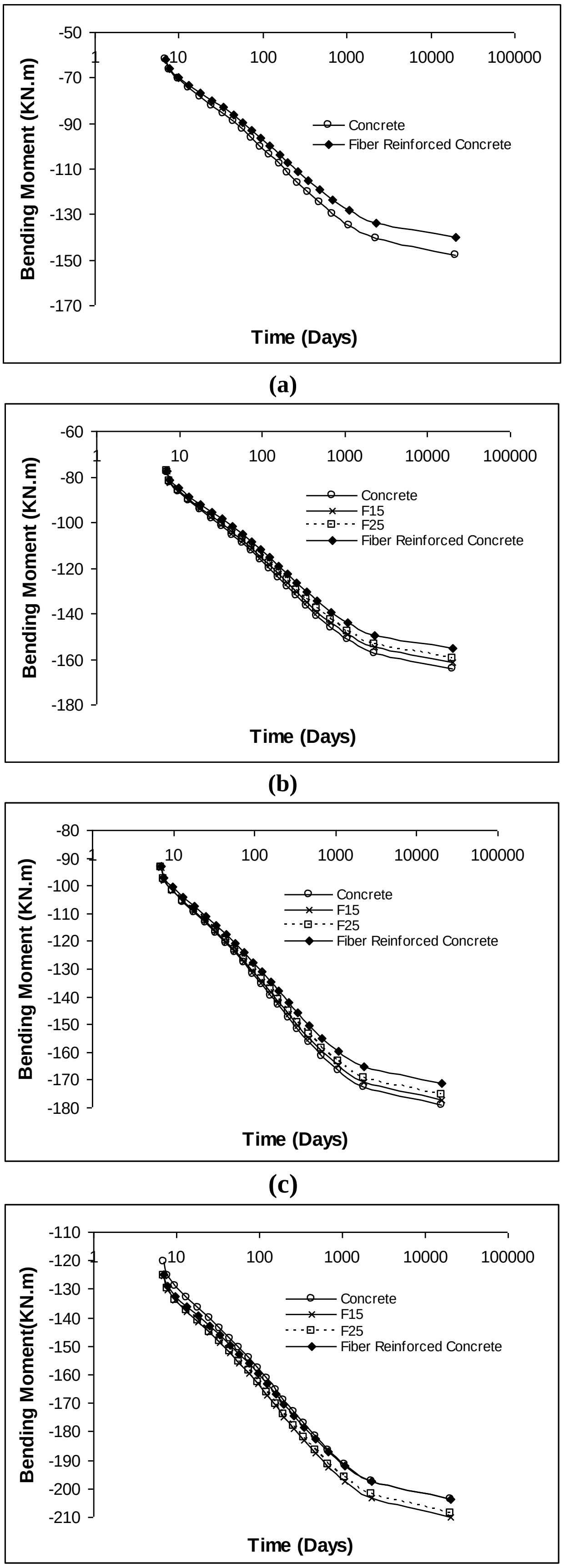

Fig. 14 Time-dependent variation of bending moment at right end of span CD: (a) $w = w_{er}$, (b) $w = 1.25w_{cr}$, (c) $w = 1.50w_{cr}$ and (d) $w = 2.0w_{cr}$

5. Conclusions

In the present paper, an efficient and novel strategy has been proposed by use of FRC in limited length near interior supports of the steel-concrete composite continuous beam. For this purpose, the hybrid analytical-numerical procedure (Chaudhary *et al.* 2007) has been further improved and generalized to make it applicable for composite beams having spans with different material properties along the length. Through numerical studies, the results for the composite beams containing steel FRC applied for different lengths in the hogging moment regions are compared with those for conventional concrete (no steel fibers content). Following important conclusions are drawn:

(i) The procedure is quite computationally efficient since no discretisation is required along the length and across the cross-section even though material changing within the span.

(ii) The proposed efficient and novel strategy of using FRC in small portion only is adequate to control the cracking, creep and shrinkage effects. The proposed strategy also enhances the service life due to significant reduction in cracked lengths, bending moments and deflections.

(iii) Use of FRC even in small length (15% of the span length) near interior supports can lead to significant reduction in cracked lengths (100% for smaller loading and approximate 60% for higher loading case) as well as in mid-span deflections up to 16%.

(iv) The benefits achieved by providing FRC over entire span are not significantly more as compared to the use of FRC in certain length near interior supports in composite structures.

As a future research work, artificial neural networks may be employed for realizing the proposed hybrid scheme in the practice. A large number of data sets may be obtained using the hybrid procedure and the networks may be developed for predicting the behaviour of composite beams containing the fiber reinforced concrete in particular locations. The proposed strategy has been successfully demonstrated by the authors earlier (Chaudhary *et al.* 2014, Gupta *et al.* 2013, 2015, Pendharkar *et al.* 2010, 2011, 2015, 2017a, b, Ramnavas *et al.* 2017, Tadesse *et al.* 2012).

References

Ashour, S.A., Wafa, F.F. and Kamal, M.I. (2000), "Effect of the concrete compressive strength and tensile reinforcement ratio on the flexural behavior of fibrous concrete beams", *Eng. Struct.*, **22**(9), 1145-1158. https://doi.org/10.1016/S0141-0296(99)00052-8.

Bazant, Z.P. (1972), "Prediction of concrete creep effects using age-adjusted effective", *ACI J. P.*, **69**(4), 212-217.

Chaudhary, S., Pendharkar, U. and Nagpal, A.K. (2007), "An analytical-numerical procedure for cracking and time-dependent effects in continuous composite beams under service load", *Steel Comp. Struct.*, **7**(3), 219-240. https://doi.org/10.12989/scs.2007.7.3.219.

Chaudhary, S., Pendharkar, U. and Nagpal, A.K. (2009), "Control of creep and shrinkage effects in steel concrete composite bridges with precast decks", *J. Bridge Eng.*, **14**(5), 336-345. https://doi.org/10.1061/(ASCE)1084-0702(2009)14:5(336).

Chaudhary, S., Pendharkar, U., Patel, K.A. and Nagpal, A.K. (2014), "Neural networks for deflections in continuous composite beams considering concrete cracking", *Iran. J. Sci. Technol. T. Civ. Eng*., **38**(C1+), 205-221.

Chern, J.C. and Young, C.H. (1989), "Compressive creep and shrinkage of steel fibre reinforced concrete", *Int. J. Cement Comp. Lightweight Concrete*, **11**(4), 205-214. https://doi.org/10.1016/0262-5075(89)90100-0.

Chern, J.C. and Young, C.H. (1990), "Factors influencing the drying shrinkage of steel fiber reinforced concrete", *ACI Mater. J*., **87**(2), 123-139.

Comite´ Euro International du Beton-Fe´de´ration International de la Pre´contrainte (CEB-FIP) (1990), Model code for concrete structures, CEB-FIP; London, United Kingdom.

Eurocode 2 (1992), Design of Concrete Structures. Part 1: General Rules and Rules for Buildings, European Committee for Standardization; Brussels, Belgium.

Fédération Internationale de Béton (FIB) (1999), Structural concrete: Textbook on behaviour, design and performance, updated knowledge of the CEB-FIP model code 1990, FIB; Lausanne, Switzerland.

Gholamhoseini, A., Khanlou, A., MacRae, G., Scott, A., Hicks, S. and Leon, R. (2016), "An experimental study on strength and serviceability of reinforced and steel fibre reinforced concrete (SFRC) continuous composite slabs", *Eng. Struct*., **114**, 171-180. https://doi.org/10.1016/j.engstruct.2016.02.010.

Grzybowski, M. and Shah, S.P. (1989), "Model to predict cracking in fibre reinforced concrete due to restrained shrinkage", *Mag. Concrete Res*., **41**(148), 125-135. https://doi.org/10.1680/macr.1989.41.148.125.

Grzybowski, M. and Shah, S.P. (1990), "Shrinkage cracking of fiber reinforced concrete", *ACI Mater. J*., **87**(2), 138-148.

Gupta, R.K., Kumar, S., Patel, K.A., Chaudhary, S. and Nagpal, A.K. (2015), "Rapid prediction of deflections in multi-span continuous composite bridges using neural networks", *Int. J. Steel Struct*., **15**(4), 893-909. https://doi.org/10.1007/s13296-015-1211-9.

Gupta, R.K., Patel, K.A., Chaudhary, S. and Nagpal, A.K. (2013), "Closed form solution for deflection of flexible composite bridges", *Procedia Engineer*., 51, 75-83. https://doi.org/10.1016/j.proeng.2013.01.013.

Haddad, R.H. and Smadi, M.M. (2004), "Role of fibers in controlling unrestrained expansion and arresting cracking in Portland cement concrete undergoing alkali-silica reaction", *Cement Concrete Res*., **34**(1), 103-108. https://doi.org/10.1016/S0008-8846(03)00245-X.

Hamoda, A., Hossain, K.M.A., Sennah, K., Shoukry, M. and Mahmoud, Z. (2017), "Behaviour of composite high performance concrete slab on steel I-beams subjected to static hogging moment", *Eng. Struct*., **140**, 51-65. https://doi.org/10.1016/j.engstruct.2017.02.030.

Johnston, C.D. (2014), Fiber-reinforced Cements and Concretes, CRC Press, Boca Raton, Florida, United States.

Kwak, H.G. and Seo, Y.J. (2002), "Shrinkage cracking at interior supports of continuous pre-cast pre-stressed concrete girder bridges", *Constr. Build. Mater*., **16**(1), 35-47. https://doi.org/10.1016/S0950-0618(01)00028-9.

Kwon, S.H. and Shah, S.P. (2008), "Prediction of early-age cracking of fiber-reinforced concrete due to restrained shrinkage", *ACI Mater. J*., **105**(4), 381-389.

Lin, W., Yoda, T. and Taniguchi, N. (2014), "Application of SFRC in steel–concrete composite beams subjected to hogging moment", *J. Constr. Steel Res*., **101**(2), 175-183. https://doi.org/10.1016/j.jcsr.2014.05.008.

Malmberg, B.O. (1978), "Method of studying the cracking of fiber concrete under restrained shrinkage", *Testing and Test Method of Fiber Cement Composites*, RILEM Symposium, Paris.

Mohammadhassani, M., Nezamabadi-Pour, H., Jumaat, M.Z., Jameel, M., Hakim, S.J.S. and Zargar, M. (2013a), "Application of the ANFIS model in deflection prediction of concrete deep beam", *Struct. Eng. Mech*., **45**(3), 319-332. http://doi.org/10.12989/sem.2013.45.3.323.

Mohammadhassani, M., Nezamabadi-Pour, H., Suhatril, M. and Shariati, M. (2013b), "Identification of a suitable ANN architecture in predicting strain in tie section of concrete deep beams", *Struct. Eng. Mech*., **46**(6), 853-868. http://doi.org/10.12989/sem.2013.46.6.853.

Nataraja, M.C., Dhang, N. and Gupta, A.P. (1999), "Stress-strain curves for steel-fiber reinforced concrete under compression", *Cement Concrete Comp*., **21**(5-6), 383-390. https://doi.org/10.1016/S0958-9465(99)00021-9.

Olesen, J.F. (2001), "Fictitious crack propagation in fiber-reinforced concrete beams", *J. Eng. Mech*., **127**(3), 272-280. https://doi.org/10.1061/(ASCE)0733-9399(2001)127:3(272).

Patel, K.A., Chaudhary, S. and Nagpal, A.K. (2016), "A tension stiffening model for analysis of reinforced concrete flexural members subjected to service load", *Comput. Concrete*, **17**(1), 29-51. https://doi.org/10.1016/j.engstruct.2007.12.022.

Pendharkar, U., Chaudhary, S. and Nagpal, A.K. (2010), "Neural networks for inelastic mid-span deflections in continuous composite beams", *Struct. Eng. Mech*., **36**(2), 165-179. https://doi.org/10.12989/sem.2010.36.2.165.

Pendharkar, U., Chaudhary, S. and Nagpal, A.K. (2011), "Prediction of moments in composite frames considering cracking and time effects using neural network models", *Struct. Eng. Mech*., **39**(2), 267-285. https://doi.org/10.12989/sem.2011.39.2.267.

Pendharkar, U., Patel, K.A., Chaudhary, S. and Nagpal, A.K. (2015), "Rapid prediction of long-term deflections in composite frames", *Steel Compos. Struct*., **18**(3), 547-563. https://doi.org/10.12989/scs.2015.18.3.547.

Pendharkar, U., Patel, K.A., Chaudhary, S. and Nagpal, A.K. (2017a), "Closed-form expressions for long-term deflections in high-rise composite frames", *Int. J. Steel Struct*., **17**(1), 31-42. https://doi.org/10.1007/s13296-016-0115-7.

Pendharkar, U., Patel, K.A., Chaudhary, S. and Nagpal, A.K. (2017b), "Rapid prediction of moments in high-rise composite frames considering cracking and time-effects", *Period. Polytech. Civ*., **61**(2), 282-291. https://doi.org/10.3311/PPci.8210.

Ramnavas, M.P., Patel, K.A., Chaudhary, S. and Nagpal, A.K. (2017), "Explicit expressions for inelastic design quantities in composite frames considering effects of nearby columns and floors", *Struct. Eng. Mech*., **64**(4), 437-447. https://doi.org/10.12989/sem.2017.64.4.437.

Ryu, H.K., Chang, S.P., Kim, Y.J. and Kim, B.S. (2005), "Crack control of a steel and concrete composite plate girder with prefabricated slabs under hogging moments", *Eng. Struct*., **27**(11), 1613-1624. https://doi.org/10.1016/j.engstruct.2005.05.015.

Ryu, H.K., Kim, Y.J. and Chang, S.P. (2007), "Crack control of a continuous composite two-girder bridge with prefabricated slabs under static and fatigue loads", *Eng. Struct*., **29**(6), 851-864. https://doi.org/10.1016/j.engstruct.2006.06.021.

Sargaphuti, M., Shah, S.P. and Vinson, K.D. (1993), "Shrinkage cracking and durability characteristics of cellulose fiber reinforced concrete", *ACI Mater. J*., **90**(4), 309-318.

Sryh, L.S.M. (2017), "Long-term flexural performance of cracked reinforced concrete beams incorporating recycled aggregate and steel fibres", PhD Dissertation, University of Leeds, Leeds, United Kingdom.

Swamy, R.N. and Stavrides, H. (1979), "Influence of fiber reinforced on restrained shrinkage and cracking", *ACI J. P*., **76**(3), 443-460.

Tadesse, Z., Patel, K.A., Chaudhary, S. and Nagpal, A.K. (2012), "Neural networks for prediction of deflection in composite bridges", *J. Constr. Steel Res.*, **68**(1), 138-149. https://doi.org/10.1016/j.jcsr.2011.08.003.

Tan, K.H. and Saha, M.K. (2005), "Ten-year study on steel fiber-reinforced concrete beams under sustained loads", *ACI Struct. J.*, **102**(3), 472-480.

Tan, K.H., Paramasivam, P. and Tan, K.C. (1994), "Instantaneous and long-term deflections of steel fiber reinforced concrete beams", *ACI Struct. J.*, **91**(4), 384-393.

Tan, K.H., Paramasivam, P. and Tan, K.C. (1995), "Cracking characteristics of reinforced steel fiber concrete beams under short-and long-term loadings", *Adv. Cem. Based Mater.*, **2**(4), 127-137. https://doi.org/10.1016/1065-7355(95)90013-6.

Tang, C.W. (2017), "Fire resistance of high strength fiber reinforced concrete filled box columns", *Steel Comp. Struct.*, **23**(5), 611-621. https://doi.org/10.12989/scs.2017.23.5.611.

Varshney, L.K., Patel, K.A., Chaudhary, S. and Nagpal, A.K. (2013), "Control of time-dependent effects in steel-concrete composite frames", *Int. J. Steel Struct.*, **13**(4), 589-606. https://doi.org/10.1007/s13296-013-4002-1.

Wang, W.W. and Dai, J.G. (2013), "Self-stressed steel fiber reinforced concrete as negative moment connection for strengthening of multi-span simply-supported girder bridges", *Adv. Struct. Eng.*, **16**(6), 1113-1127. https://doi.org/10.1260/1369-4332.16.6.1113.

Wang, W.W., Dai, J.G., Guo, L. and Huang, C.K. (2011), "Long-term behavior of prestressed old-new concrete composites beams", *J. Bridge Eng.*, **16**(2), 275-285.

Zhang, J. (2003), "Modeling of the influence of fibers on creep of fiber reinforced cementitious composite", *Compos. Sci. Technol.*, **63**(13), 1877-1884. https://doi.org/10.1016/S0266-3538(03)00160-X.

Zhao, G., Di Prisco, M. and Vandewalle, L. (2015), "Experimental investigation on uniaxial tensile creep behavior of cracked steel fiber reinforced concrete", *Mater. Struct.*, **48**(10), 3173-3185. https://doi.org/10.1617/s11527-014-0389-1.

Zollo, R.F. (1997), "Fiber-reinforced concrete: an overview after 30 years of development", *Cement Concrete Comp.*, **19**(2), 107-122. https://doi.org/10.1016/S0958-9465(96)00046-7.

CC

Appendix A1: Values for Figs. 10, 13 and 14

Table A1 Values for Fig. 10

Time (days)	Mid-span deflection (mm)															
	(a) $w = w_{cr}$				(b) $w = 1.25w_{cr}$				(c) $w = 1.50w_{cr}$				(d) $w = 2.0w_{cr}$			
	Concrete	F15	F25	FRC	Concrete	F15	F25	FRC	Concrete	F15	F25	FRC	Concrete	F15	F25	FRC
7	2.07	2.06	2.06	2.03	2.66	2.58	2.57	2.54	3.30	3.10	3.10	3.05	4.57	4.33	4.33	4.26
7.7	2.35	2.34	2.34	2.26	3.00	2.90	2.90	2.80	3.68	3.47	3.47	3.36	5.05	4.79	4.79	4.64
9.7	2.54	2.52	2.52	2.41	3.20	3.10	3.10	2.97	3.91	3.69	3.69	3.54	5.33	5.06	5.05	4.86
13.1	2.70	2.69	2.69	2.54	3.39	3.28	3.28	3.12	4.12	3.89	3.88	3.70	5.58	5.29	5.29	5.06
18	2.85	2.84	2.84	2.67	3.56	3.45	3.45	3.26	4.31	4.07	4.07	3.85	5.82	5.50	5.50	5.24
25	3.01	3.00	3.00	2.80	3.74	3.61	3.61	3.40	4.51	4.25	4.25	4.00	6.05	5.72	5.72	5.42
33.4	3.15	3.14	3.14	2.92	3.89	3.77	3.77	3.52	4.68	4.41	4.41	4.14	6.25	5.91	5.91	5.58
44.5	3.30	3.28	3.28	3.04	4.06	3.92	3.92	3.65	4.86	4.58	4.58	4.28	6.46	6.10	6.10	5.74
57.5	3.43	3.42	3.42	3.16	4.21	4.07	4.07	3.78	5.03	4.73	4.73	4.41	6.66	6.28	6.28	5.90
74	3.57	3.56	3.56	3.27	4.36	4.22	4.22	3.90	5.20	4.89	4.89	4.54	6.86	6.47	6.46	6.05
95.5	3.71	3.71	3.71	3.40	4.52	4.37	4.37	4.03	5.37	5.05	5.05	4.68	7.06	6.66	6.65	6.21
122	3.86	3.85	3.85	3.52	4.68	4.52	4.52	4.16	5.54	5.22	5.22	4.82	7.26	6.84	6.84	6.37
157.5	4.01	4.00	4.01	3.65	4.84	4.69	4.69	4.29	5.73	5.39	5.39	4.96	7.47	7.04	7.04	6.54
199	4.15	4.15	4.15	3.77	5.00	4.83	4.84	4.42	5.90	5.54	5.54	5.09	7.67	7.22	7.22	6.69
261	4.31	4.31	4.31	3.90	5.17	5.00	5.01	4.56	6.09	5.72	5.72	5.24	7.89	7.42	7.42	6.87
343	4.47	4.47	4.47	4.04	5.34	5.17	5.17	4.70	6.27	5.90	5.90	5.39	8.10	7.62	7.62	7.03
468	4.64	4.64	4.64	4.18	5.53	5.35	5.35	4.85	6.47	6.08	6.08	5.55	8.33	7.83	7.83	7.22
683	4.82	4.82	4.83	4.34	5.73	5.54	5.55	5.02	6.69	6.28	6.29	5.72	8.58	8.06	8.06	7.41
1073	5.01	5.01	5.02	4.50	5.93	5.74	5.74	5.18	6.91	6.49	6.49	5.89	8.83	8.29	8.30	7.61
2253	5.23	5.23	5.24	4.68	6.17	5.96	5.97	5.37	7.17	6.73	6.73	6.09	9.12	8.56	8.56	7.84
20000	5.46	5.46	5.47	4.87	6.41	6.20	6.21	5.58	7.44	6.97	6.98	6.30	9.42	8.84	8.85	8.08

Table A2 Values for Fig. 13

Time (days)	Bending moment (kNm)													
	(a) $w = w_{cr}$		(b) $w = 1.25w_{cr}$				(c) $w = 1.50w_{cr}$				(d) $w = 2.0w_{cr}$			
	Concrete	FRC	Concrete	F15	F25	FRC	Concrete	F15	F25	FRC	Concrete	F15	F25	FRC
7	-82.46	-82.53	-99.96	-103.65	-103.72	-103.16	-115.77	-123.88	-123.95	-123.34	-146.40	-157.20	-157.25	-156.56
7.7	-88.69	-87.98	-106.28	-110.06	-110.05	-108.61	-122.29	-130.39	-130.38	-128.81	-153.47	-164.24	-164.22	-162.39
9.7	-94.02	-92.73	-111.51	-115.38	-115.29	-113.37	-127.41	-135.72	-135.64	-133.56	-158.50	-169.52	-169.43	-167.05
13.1	-99.14	-97.33	-116.51	-120.47	-120.31	-117.97	-132.28	-140.82	-140.67	-138.15	-163.21	-174.52	-174.37	-171.50
18	-104.09	-101.81	-121.34	-125.39	-125.17	-122.44	-136.97	-145.74	-145.53	-142.61	-167.71	-179.32	-179.10	-175.81
25	-109.24	-106.48	-126.36	-130.50	-130.21	-127.11	-141.84	-150.85	-150.57	-147.27	-172.37	-184.28	-184.00	-180.30
33.4	-113.94	-110.76	-130.95	-135.17	-134.82	-131.39	-146.29	-155.51	-155.19	-151.54	-176.63	-188.81	-188.47	-184.42
44.5	-118.90	-115.27	-135.77	-140.08	-139.67	-135.91	-150.97	-160.42	-160.03	-156.04	-181.10	-193.57	-193.17	-188.75
57.5	-123.52	-119.50	-140.28	-144.67	-144.20	-140.13	-155.33	-165.00	-164.56	-160.26	-185.26	-198.01	-197.55	-192.81
74	-128.34	-123.91	-144.97	-149.44	-148.92	-144.54	-159.88	-169.77	-169.27	-164.66	-189.60	-202.63	-202.11	-197.04
95.5	-133.43	-128.58	-149.93	-154.48	-153.90	-149.21	-164.68	-174.81	-174.25	-169.31	-194.16	-207.50	-206.92	-201.51
122	-138.46	-133.20	-154.83	-159.47	-158.83	-153.83	-169.42	-179.78	-179.17	-173.92	-198.68	-212.31	-211.68	-205.94
157.5	-143.85	-138.16	-160.09	-164.81	-164.11	-158.79	-174.51	-185.12	-184.45	-178.87	-203.51	-217.46	-216.77	-210.69
199	-148.77	-142.70	-164.87	-169.68	-168.93	-163.33	-179.14	-189.98	-189.25	-183.39	-207.91	-222.16	-221.41	-215.04
261	-154.56	-148.03	-170.51	-175.41	-174.60	-168.66	-184.59	-195.70	-194.91	-188.71	-213.07	-227.67	-226.86	-220.13
343	-160.12	-153.18	-175.93	-180.93	-180.06	-173.81	-189.84	-201.21	-200.36	-193.84	-218.05	-232.98	-232.11	-225.07
468	-166.20	-158.80	-181.84	-186.95	-186.01	-179.43	-195.55	-207.21	-206.30	-199.44	-223.46	-238.76	-237.82	-230.43
683	-172.86	-164.96	-188.33	-193.55	-192.54	-185.60	-201.81	-213.79	-212.81	-205.59	-229.38	-245.09	-244.09	-236.32
1073	-179.55	-171.17	-194.84	-200.17	-199.09	-191.80	-208.10	-220.40	-219.35	-211.78	-235.33	-251.45	-250.37	-242.24
2253	-187.62	-178.62	-202.68	-208.15	-206.99	-199.26	-215.66	-228.36	-227.23	-219.21	-242.44	-259.08	-257.92	-249.33
20000	-195.00	-186.67	-211.14	-216.78	-215.51	-207.30	-223.80	-236.96	-235.73	-227.23	-250.08	-267.31	-266.04	-256.96

Table A3 Values for Fig. 14

Time (days)	Bending moment (kNm)													
	(a) $w = w_{cr}$		(b) $w = 1.25w_{cr}$				(c) $w = 1.50w_{cr}$				(d) $w = 2.0w_{cr}$			
	Concrete	**FRC**	**Concrete**	**F15**	**F25**	**FRC**	**Concrete**	**F15**	**F25**	**FRC**	**Concrete**	**F15**	**F25**	**FRC**
7	-61.91	-61.89	-77.98	-77.59	-77.60	-77.37	-93.29	-93.21	-93.22	-92.93	-120.31	-125.34	-125.35	-124.97
7.7	-66.58	-65.98	-82.63	-82.26	-82.15	-81.46	-97.95	-97.91	-97.80	-97.01	-125.19	-130.06	-129.97	-129.01
9.7	-70.58	-69.55	-86.65	-86.18	-85.98	-85.02	-101.96	-101.84	-101.65	-100.58	-129.12	-134.03	-133.85	-132.59
13.1	-74.42	-73.00	-90.52	-89.94	-89.66	-88.47	-105.81	-105.61	-105.34	-104.04	-132.86	-137.84	-137.58	-136.06
18	-78.14	-76.36	-94.26	-93.58	-93.23	-91.83	-109.54	-109.26	-108.91	-107.40	-136.48	-141.52	-141.19	-139.44
25	-82.00	-79.86	-98.15	-97.35	-96.93	-95.33	-113.42	-113.05	-112.63	-110.90	-140.24	-145.34	-144.94	-142.96
33.4	-85.53	-83.07	-101.70	-100.81	-100.32	-98.54	-116.96	-116.51	-116.02	-114.11	-143.67	-148.83	-148.37	-146.20
44.5	-89.25	-86.46	-105.44	-104.45	-103.89	-101.93	-120.69	-120.15	-119.60	-117.50	-147.27	-152.51	-151.97	-149.61
57.5	-92.72	-89.63	-108.93	-107.84	-107.22	-105.10	-124.17	-123.55	-122.93	-120.67	-150.64	-155.93	-155.34	-152.80
74	-96.34	-92.93	-112.58	-111.37	-110.69	-108.41	-127.80	-127.09	-126.41	-123.98	-154.15	-159.51	-158.85	-156.14
95.5	-100.16	-96.43	-116.42	-115.11	-114.36	-111.91	-131.64	-130.83	-130.09	-127.49	-157.85	-163.28	-162.56	-159.66
122	-103.93	-99.90	-120.22	-118.80	-117.99	-115.37	-135.43	-134.53	-133.72	-130.95	-161.51	-167.01	-166.22	-163.15
157.5	-107.98	-103.62	-124.30	-122.76	-121.88	-119.10	-139.49	-138.50	-137.62	-134.68	-165.44	-171.01	-170.16	-166.90
199	-111.67	-107.02	-128.01	-126.37	-125.43	-122.50	-143.19	-142.11	-141.18	-138.08	-169.01	-174.65	-173.74	-170.33
261	-116.01	-111.02	-132.39	-130.62	-129.60	-126.50	-147.55	-146.37	-145.36	-142.08	-173.22	-178.94	-177.96	-174.36
343	-120.19	-114.89	-136.59	-134.71	-133.63	-130.36	-151.75	-150.46	-149.39	-145.95	-177.26	-183.07	-182.02	-178.26
468	-124.75	-119.10	-141.18	-139.17	-138.02	-134.57	-156.32	-154.93	-153.78	-150.17	-181.67	-187.57	-186.45	-182.50
683	-129.75	-123.72	-146.22	-144.06	-142.83	-139.20	-161.34	-159.82	-158.60	-154.80	-186.51	-192.51	-191.31	-187.17
1073	-134.77	-128.38	-151.27	-148.97	-147.67	-143.85	-166.38	-164.74	-163.44	-159.45	-191.36	-197.47	-196.19	-191.86
2253	-140.83	-133.97	-157.37	-154.89	-153.49	-149.44	-172.46	-170.67	-169.28	-165.05	-197.21	-203.44	-202.08	-197.50
20000	-147.65	-140.00	-163.97	-161.29	-159.78	-155.48	-179.04	-177.08	-175.57	-171.09	-203.51	-209.91	-208.43	-203.59